Laser Raman microprobe analysis of graphite exposed to edge plasma in the TEXTOR tokamak

T. Hirai[1]*, J. Compan[1], K. Niwase[2], J. Linke[1]

[1] IEF 2, Forschungszentrum Jülich GmbH, EURATOM Association, 52425 Jülich, Germany

[2] Hyogo University of Teacher Educations, Hyogo, 673-1494, Japan

Abstract

We exposed an isotropic fine grain graphite (EK98) block to the edge plasma in the TEXTOR tokamak and studied by Raman spectroscopy. Raman spectra from the net erosion area and the net deposition area, where co-deposits (hard layer) were created by the tokamak discharges, are remarkably different. The former ones consist of two sharp peaks: the D-peak (≈ 1355 cm^{-1}) and the G-peak (≈ 1580 cm^{-1}). The latter are very broad ones, which are similar to the Raman spectra of amorphous carbon. Fitting analyses of the Raman spectra for the net erosion area exhibit an interesting linear relationship between the G-peak width ($FWHM_G$) and the peak intensity ratio (I_D / I_G). Comparison with the diagram given for ion-irradiated graphite revealed that thermally unstable defects of single vacancies scarcely remained due to the power loading in this plasma exposure condition but thermally stable defects such as the dislocation dipoles could be accumulated.

Keywords: graphite, Raman spectroscopy, heat load, plasma exposure, point defects

PACS codes: 28.52.-s, 28.52.Fa, 63.50.+x

***Corresponding author: T. Hirai**

Email: t.hirai@fz-juelich.de

Tel: +49 2461 61 5843

Fax: +49 2461 61 3699

Postal address:

IWV2 Forschungszentrum Juelich

52425 Juelich, Germany

1. Introduction

Carbon-based materials (CBMs) are favourable for fusion applications because of a low atomic number, good thermo-mechanical properties, low coefficient of thermal expansion and the absence of melting. Fine grain graphites are used in numerous existing fusion devices and the advanced CBMs, carbon fibre composites (CFCs), are the candidate material for the vertical targets of the ITER divertor, where heat and particle fluxes are the highest [**1**]. The high particle load causes radiation damage in CBMs which leads to a reduction of the thermal conductivity [**2**], whereas the high heat flux loads will raise the temperature of CBMs and may cause an annealing of the radiation damage.

Raman spectroscopy is sensitive to the graphitic structures (phonon distribution) [**3**], and then has been applied in order to study the structural changes of CBMs. Various CBMs, e.g. fine grain graphite, pyrolytic graphite, diamond, CFC, glassy carbon, were characterized after neutron irradiation [**4, 5**], ion implantation [**5-9**] and electron beam loading [**10, 11**] as well as the original grades [**9, 12-14**].

In the present paper, to clarify the effect of intense plasma loading on the damage accumulation for a graphite limiter, a fine grain graphite block was exposed to the edge plasma in the TEXTOR tokamak and studied by Raman spectroscopy.

2. Experimental

An isotropic fine graphite (EK98) block was machined as a test limiter, of which sizes are 120 mm in the toroidal direction and 80 mm in the poloidal direction with a spherical surface of radius 70 mm. The block was mounted on the limiter lock system and exposed to the edge plasma in the TEXTOR tokamak in Forschungszentrum Jülich. The typical plasma parameters are: the line averaged electron density n_e = 2-6 x 10^{13} m^{-3}, the plasma current I_p = 330 kA and the power of the neutral beam injection P_{NBI} = 1.8 MW. The details of the plasma exposure experiments were described elsewhere [**15**]. The graphite block was exposed to 29 discharges (5-6 seconds for each discharge, shot number #91142 - #91170) at the last closed flux surface (LCFS, r = 46 cm) and 5 mm outside of LCFS (r = 46.5 cm) in the tokamak. The typical edge plasma parameters were, $n_e \approx 2 \times 10^{18}$ m^{-3}, $T_e \approx 100$ eV. The highest ion flux and heat load at the spherical limiter surface were roughly estimated to be 7×10^{22} ions/(m^2s) and 9 MW/m^2, respectively. Then, the integrated ion fluence was estimated to be approximately 1×10^{25} ions/m^2. The limiter temperature was measured by thermocouples. The bulk temperature increased from 300 °C to 400 °C during the experimental campaign and the maximum surface temperature could reach above 1500 °C at the end of each discharge. The test limiter after the plasma exposure was investigated by micro-Raman spectroscopy, using a backscattering geometry with the 488.0 nm line of Ar-ion laser. The beam spot had a diameter of 2 µm. Although the nominal grain size of the EK98 grade is 7-12 µm, we did not take into account the micro-structure of the test limiter for the Raman measurements as the Raman spectra did not show any significant micro-scale dependence. The analysis depth (d) was calculated by the absorption coefficient (a) of the laser light in matters. The absorption coefficient of a 488 nm (2.55 eV) photon in low hydrogen-containing deposits (high density > 1.64 g/cm$^{3)}$ has been evaluated to be 6×10^6 m^{-1} [16]. Hence, the analysis depth is calculated to be 83 nm ($d = 1/(2\alpha)$). The analysis depth should be larger in deposits with the higher hydrogen contents. The analysis depth in the isotropic fine grain graphite, on the other hand, is considered to be in a range of 40–50 nm, judging from the optical skin depth of a laser with similar wavelength, 514.5 nm (2.42 eV) [17,18].

3. Results

Figure 1 shows an optical micrograph of the test limiter after the plasma exposure in the TEXTOR tokamak. The areas at the highest heat load look darker than the neighboring areas. The micro-Raman measurements were performed along the toroidal direction, shown by a scale attached on the limiter surface. Typical Raman spectra from three different areas of the plasma exposed limiter surface are shown in Fig.2. They correspond to (a) the highly loaded area at 52 mm from the limiter edge in the net erosion area, (b) the net deposition area at 20 mm from the limiter edge and (c) the rear surface of the limiter, of which result corresponds to the Raman spectra of the original graphite grade. One can find that the Raman spectra from the highly loaded area and the rear surface area exhibit two clear peaks, which correspond to the graphite peak (G-peak, E_{2g} Raman active mode) around 1580 cm^{-1} and the disordered peak (D-peak, originated by non-zero-centre phonon) around 1355 cm^{-1} [**3**]. The spectra could be deconvoluted into two sharp Lorenzian peaks with a least-squares algorithm as shown in Fig.2. The Raman spectrum from the net deposition area created by the tokamak discharges, on the other hand, exhibits a very broad feature, but can be fitted by two Gaussian peaks.

Figure 3 displays the change of Raman intensity ratio (I_D/I_G), which was deduced by the deconvolution, along the toroidal direction. The horizontal axis shows the position on the limiter surface from the ion drift side to the electron drift side. The value of I_D/I_G obtained from the rear surface of the limiter is also shown by a horizontal bar (I_D/I_G = 0.24 - 0.4) as the original grade of graphite. The central area between 3.5 and 11.5 cm corresponds to a net erosion area which was exposed to plasma more intensively as this area is closer to the plasma. The lateral edges located at the positions between 0 and 3.5 cm, 11.5 and 14 cm, on the other hand, correspond to the net deposition areas. There is a typical heat flux profile at the limiter surface due to (1) the radial decay of the heat flux in the tokamak, (2) the projection of the heat flux onto the spherical limiter surface. The largest temperature increases were observed around 5.5 cm and 9.5 cm. Rather moderate temperature increases were measured around the centre of the limiter (7.5 cm at the tangential point) and at the lateral sides of the limiter (the net deposition area).

4. Discussion

Here, we discuss the Raman spectra of the plasma exposed limiter in terms of defect formation and the effect of plasma impurities, etc. One should note that the intensity ratio of I_D/I_G in the net erosion area is higher than the value of the original grade as shown in Fig. 3. This means that the plasma exposure in the TEXTOR tokamak leads to the introduction of defects in the graphite limiter. The value of I_D/I_G for various grades of graphite has been widely accepted to have an inverse proportionality against a "crystalline size La" [**14**]. However, in the case of irradiation, the change of I_D/I_G cannot simply be explained by the change of La but by accumulation of in-plane defects of single vacancies and some in-plane defects which can induce the turbulence and disordering of the basal plane [**7, 19**]. One should note that the thermal stability of the two types of defects is different: single vacancies can mutually annihilate with interstitials by annealing below 873 K but not for the latter defects [**20**]. By assigning the latter defects as dislocation dipoles, the dimensional change and the Raman intensity ratio under irradiation could be well explained by a kinetic model [**21**]. The dislocation dipoles nucleate via the relaxation and stabilization of di-vacancies and grow linearly by knock-on process [**22**].

To clarify the nature of defects formed in the graphite limiter, we utilize the diagram of the relation between the full width at half maximum of G-peak, $FWHM_G$ and the peak intensity ratio, I_D/I_G as shown in Fig. 4. This diagram was given by a systematic investigation on the change of Raman spectra for highly oriented pyrolytic graphite (HOPG) specimens irradiated with He ions at temperatures between RT and 973 K [**5, 7**]. The dash-line corresponds to the accumulation of single vacancies due to Frenkel-pair production. The upward deviation from the dash-line corresponds to the formation of dislocation dipoles, of which accumulation induces the turbulence of the basal planes. The solid line, on the other hand, shows the change of Raman spectra for HOPG specimens irradiated above 573 K. Below 473 K, the upward deviation from the dashed line starts at higher values of I_D/I_G compared to the values above 573 K. This is originated from the lower annealing effect of Frenkel pairs, which allows single vacancies to accumulate to high concentration. Then, an increase of the I_D/I_G along the solid line means a gradual increase of the concentration of thermally stable defects of dislocation dipoles. The dotted line corresponds to the amorphization of the graphite structure [**5, 7**] due to a remarkable accumulation of dislocation dipoles [**21, 22**].

The present data on the limiter are plotted in the diagram. Notably, the data from the net erosion area follow the solid-line. This is consistent with the case of ion irradiation as the bulk temperature of the limiter graphite was estimated to be from 573 K to 673 K under the loading condition. It means that defects remained after the plasma exposures are mostly thermally stable defects, i.e. dislocation dipoles. Detailed change of I_D/I_G in the net erosion area can also be explained by the areal dependence of the bulk temperature under the plasma loading. The I_D/I_G exhibits minima at the highest power loading points and maximum around the tangential point as shown in Fig.3. This indicates that the increase of surface temperature induced by higher loads enhances the annealing of point defects, leading to the reduction of the formation of defect clusters such as dislocation dipoles.

The Raman spectra from the co-deposits created by the tokamak discharges, on the other hand, show a remarkable broad feature as shown in Fig.2 (b). According to the experiments in the past, deposits in TEXTOR grow typically in a rate of 2-3 nm/s [**23**]. Thus, the possible thickness range of deposits created by 174 s (29 shots of 6 s discharge) tokamak-discharge will be around 350-520 nm. Then, it is fair to consider that the Raman analysis was done mainly within the deposits, judging from the analysis depths for graphite and hydrogen-containing deposits. It is consistent with the spectra obtained at the net deposit area, which show no additional sharp peaks expected from the substrate graphite.

The co-deposits of hydrogen isotopes (hydrogen (H) and deuterium (D)) and carbon (C), has various properties depending on the plasma parameters and the substrate temperature. Commonly, the hydrogenated carbon deposits are classified in two groups: (i) the hard layer with high density (≈ 2.0 g/cm^3), which has a low H(D)/C ratio (≈ 0.4), and (ii) the soft (polymer-like) layer with low density (≈ 1.1 g/cm^3), which has a high H(D)/C ratio (≈ 1) [**24**]. The H(D)/C ratio of the co-deposits created at the limiter surface in similar experimental conditions are commonly around 0.4 or less [**25**]. Then, the studied co-deposits are supposed to be hard layers and the broad Raman feature should reflect a disordered carbon structure in the layer. Dedicated studies of such co-deposits could be carried out with Fourier Transform Infrared (FTIR) spectroscopy by observing directly the C-H vibrational bands [**24**].

Also, one should mention that Rutherford Backscattering Spectrometry (RBS) has revealed the existence of metallic impurities e.g. boron, copper, tungsten at the limiter surface [**15**]. These impurities were originated from the boronization as a wall-conditioning [**26**] and the simultaneous experimental program with a test limiter made out of a castellated W/Cu [**15**]. However, we could not find any significant feature of the metallic elements in the Raman spectra.

5. Conclusions

A test limiter, which was made of fine graphite and exposed to the edge plasma in the TEXTOR tokamak, was observed by Raman spectroscopy for the first time. The net erosion area and the net deposition area are clearly classified by the shape of Raman spectra. The Raman spectra in the former area consist of sharp Lorenzian peaks but of broad Gaussian peaks in the latter area. Detailed analysis on the Raman spectra from the net erosion area indicates that the defects remained after the plasma exposures are mostly thermally stable defects, i.e. the dislocation dipoles. This is probably due to the increase of surface temperature by the plasma exposure, enhancing the annihilation of thermally unstable point defects of single vacancies with interstitials. The broad Raman feature from the net deposition area reflect a disordered graphitic structure, which is originated from hard layers of co-deposition of hydrogen isotopes and carbon.

Acknowledgements

Authors would like to thank Drs. G. Sergienko and A. Kreter for discussions on the plasma exposure experiments in the TEXTOR tokamak.

References

[1] T. Hirai, K. Ezato, P. Majerus, Mater. Trans. 46 (2005) 412-424.

[2] M. Roedig, W. Kuehnlein, J. Linke, D. Pitzer, M. Merola, E. Rigal, B.Schedler, E. Visca, J. Nucl. Mater. 329-3 (2004) 766-770.

[3] R. Al-Jishi, G. Dresselhaus, Phys. Rev. B 26 (1982) 4514-4522.

[4] K. Niwase, K. Nakamura, T. Shikama, T. Tanabe, 170 (1990) 106-108.

[5] T. Tanabe, T. Maruyama, M. Iseki, K. Niwase, H. Atsumi, Fusion Eng. Design. 29 (1995) 428-434.

[6] E.S. Elman, M. Shayegan, M. S. Dresselhaus, H. Mazurek, G. Dresselhaus, Phys. Rev. B 25 (1982) 4142-4156.

[7] K. Niwase, T. Tanabe, Mater. Trans. 34 (1993) 1111-1121.

[8] K. Niwase, Y. Kakimoto, I. Tanaka, T. Tanabe, Nucl. Instr. Meth. in Phys. Res. B 91 (1994) 78-82.
[9] N. Kangai, T. Tanabe, K. Niwase, J. Nucl. Mater. 212-215 (1994) 1234-1238.
[10] M. Kitajima, M. Fujitsuka, H. Shinno, J. Mater. Science letters 9 (1990) 19-21.
[11] T. Tanabe, K. Niwase, Y. Miyamoto, I. Tanaka, M. Seki, M. Akiba, M. Arai, H. Shinno, M. Fujitsuka, Y. Kubota, J. Nucl. Mater. 176-177 (1990) 467-472.
[12] K. Ashida, K. Kanamori, K. Watanabe, J. Vac. Sci. Technol. A6 (1988) 2232-2237.
[13] T. Tanabe, K. Niwase, N. Tsukuda, E. kuramoto, J. Nucl. Mater. 191-194 (1992) 330-334.
[14] F. Tunstra, J.L.Koenig, J. Chemical Physics 53 (1970) 1126-1130.
[15] T. Hirai, V. Philipps, A. Huber, G. Sergienko, J. Linke, T. Wakui, T. Tanabe, M. Rubel, M. Wada, T. Ohgo et al., J. Nucl. Mater. 313-316 (2003) 69-73.
[16] F. W. Smith, J. Appl. Phys., Vol. 55 (1984) 764-771.
[17] D. -Q. Yang, E. Sacher, Surface Science 504 (2002) 125-137.
[18] J. Liu, M. D. Hou, C. Trautmann, R. Neumann, C. Müller, Z. G. Wang, Q. X. Zhang, Y. M. Sun, Y. F. Jin, H. W. Liu, H. J. Gao, Nucl. Instr. and Meth. B 212 (2003) 303-307.
[19] K. Niwase, Phys. Rev. B 52 (1995) 15785-15798.
[20] K. Niwase, I. Tanaka, T. Tanabe, J. Nucl. Mater. 191-194 (1992) 335.
[21] K. Niwase, Phil. Mag. Let. 82 (2002) 401-408.
[22] K. Niwase, Materials Science and Engineering A 400 – 401 (2005) 101-104.
[23] P. Wienhold, M. Rubel, M. Mayer, D. Hildebrandt, W. Schneider, A. Kirschner, Phys. Scr. T94 (2001) 141-145.
[24] W. Jacob, Thin Solid Films 326 (1998) 1-42.
[25] V. Philipps, A. Pospieszczyk, A. Huber, A. Kirschner, J. Rapp, B. Schweer, P. Wienhold, G. van Oost, G. Sergienko, T. Tanabe, K. Ohya, M. Wada, T. Ohgo and M. Rubel, J. Nucl. Mater. 258-263 (1998) 858-864.
[26] J. Winter, H.G.Esser, L.Könen, V. Philipps, H.Reimer, J. v. Seggern, J. Schlüter, E. Vietzke, F. Waelbroeck, P. Wienhold, T. Banno, D. Ringer, S. Veprek, J. Nucl. Mater. 162-164 (1989) 713-723.

Figure caption

Figure 1 Image of a test limiter exposed to the edge plasma in the TEXTOR tokamak. A scale is attached for positioning of micro-Raman measurements.

Figure 2 Typical Raman spectra from the graphite limiter surfaces of (a) the highly loaded area in the net erosion area, (b) the net deposition area, (c) the rear side of the graphite limiter, indicating spectrum from the original grade.

Figure 3 Variation of Raman intensity ratios (I_D / I_G) of the graphite limiter along the toroidal direction after the plasma exposure.

Figure 4 Diagram of the change in peak width of G-peak ($FWHM_G$) and the intensity ratio (I_D / I_G) on irradiation [**5, 7**]. The diagram has been analyzed in terms of the formation of single vacancies and disordered regions (dislocation dipoles) [**18**]. The present data are plotted in the diagram.

Figure 1

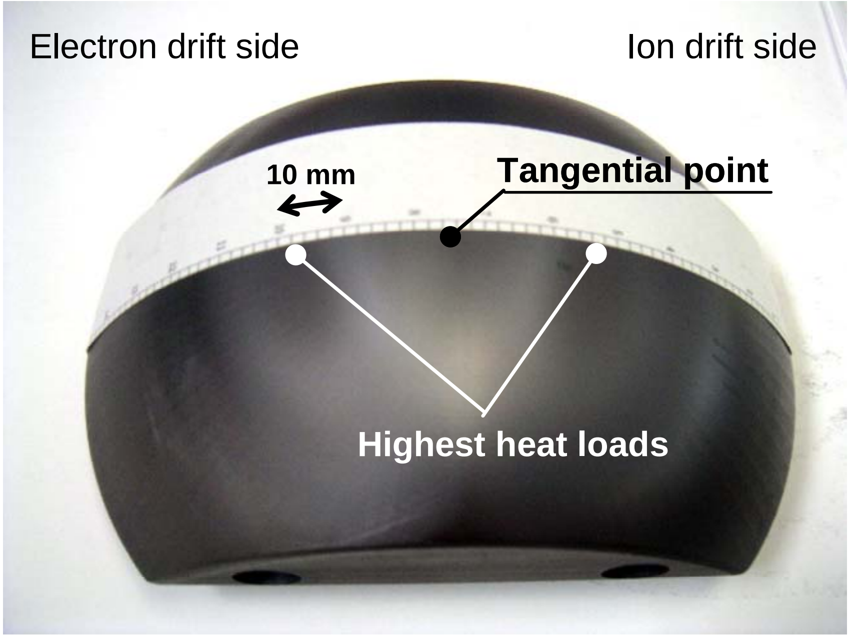
Electron drift side
Ion drift side
10 mm
Tangential point
Highest heat loads

Figure 2

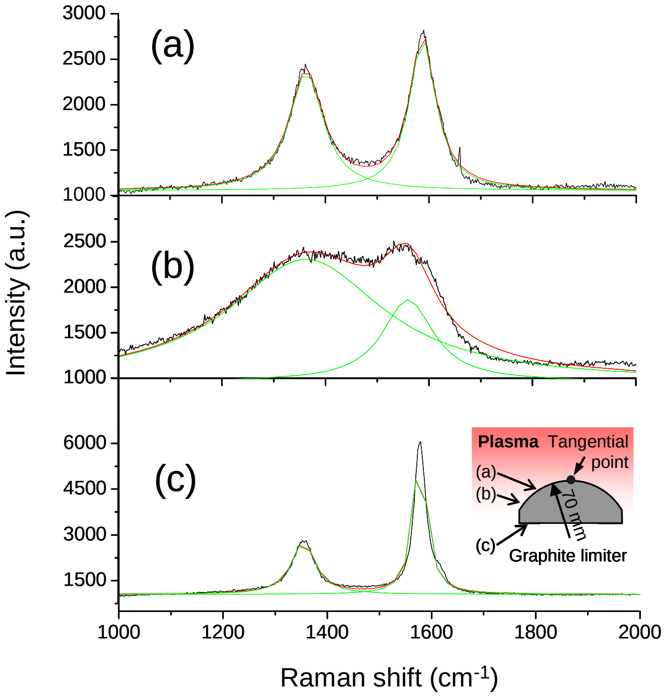

3000
2500
2000
1500
1000
(a)
2500
2000
1500
1000
(b)
Intensity (a.u.)
6000
4500
3000
1500
(c)
Plasma
Tangential point
(a)
(b)
(c)
70 mm
Graphite limiter
1000
1200
1400
1600
1800
2000
Raman shift (cm-1)

Figure 3

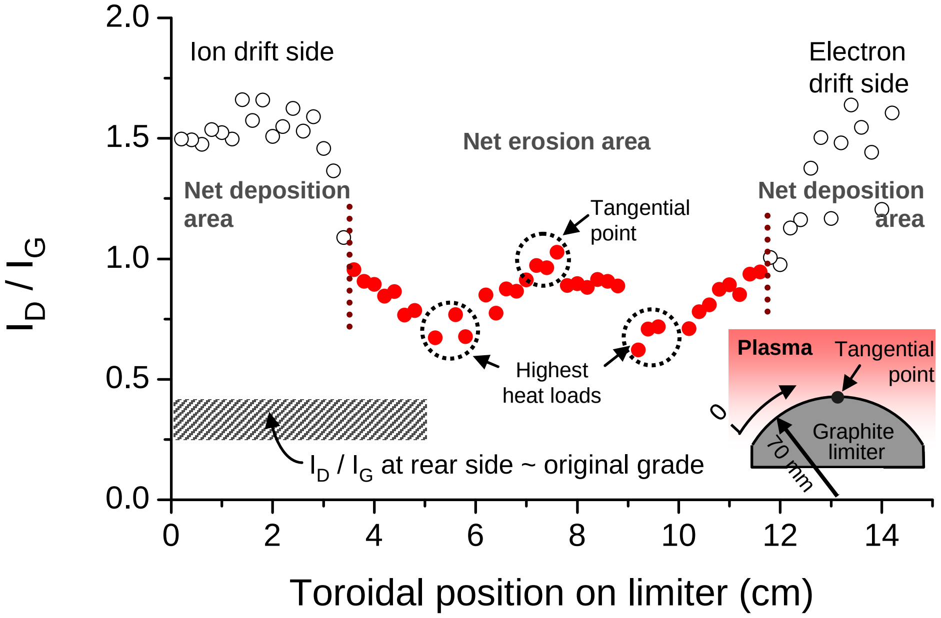
2.0
1.5
1.0
0.5
0.0
0
2
4
6
8
10
12
14
I_D / I_G
Toroidal position on limiter (cm)
Ion drift side
Electron drift side
Net erosion area
Net deposition area
Net deposition area
Tangential point
Highest heat loads
I_D / I_G at rear side ~ original grade
Plasma
Tangential point
0
70 mm
Graphite limiter

Figure 4

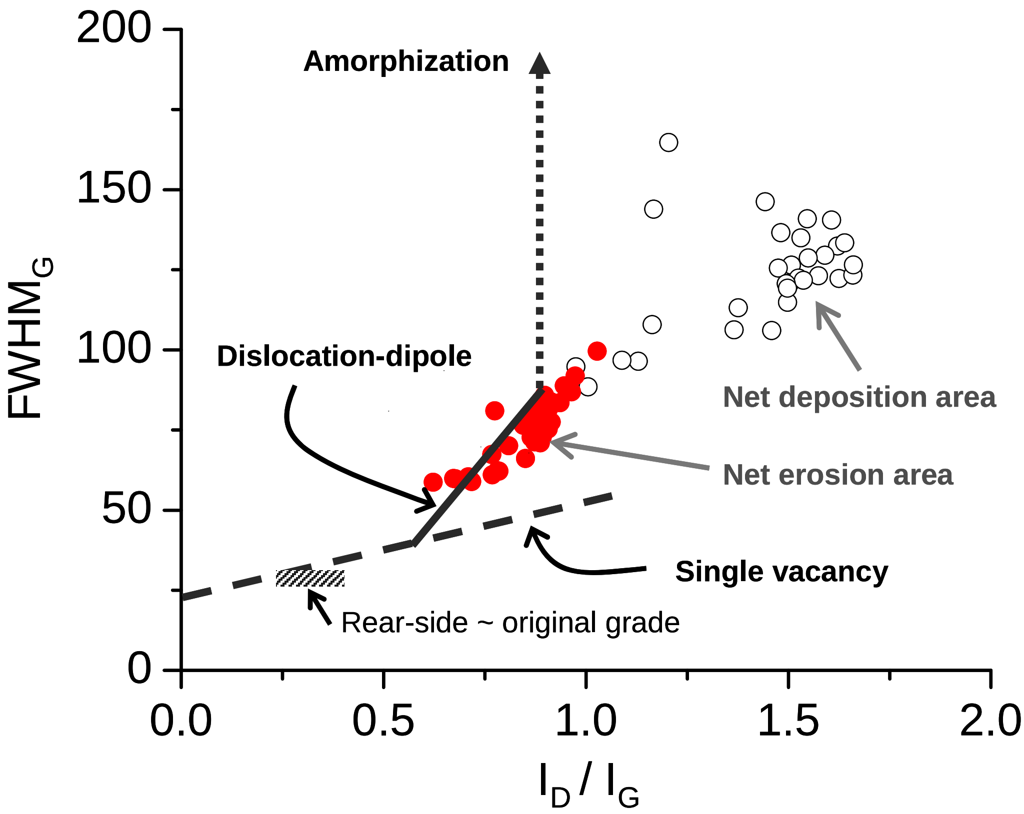

200
150
100
50
0
FWHM_G
Amorphization
Dislocation-dipole
Net deposition area
Net erosion area
Single vacancy
Rear-side ~ original grade
0.0
0.5
1.0
1.5
2.0
I_D / I_G